Experimental Neurology 370 (2023) 114581

Contents lists available at ScienceDirect

Experimental Neurology

journal homepage: www.elsevier.com/locate/yexnr

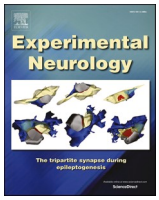

Research paper

Transcranial static magnetic stimulation reduces seizures in a mouse model of Dravet syndrome

C. Rivadulla [a,b,c,*], J.L. Pardo-Vazquez [a,b,c], C. de Labra [a,b,d], J. Aguilar [e], E. Suarez [f], C. Paz [f], M. Álvarez-Dolado [g], J. Cudeiro [a,b,c,h]

[a] Universidade da Coruña, NEUROcom, Centro Interdisciplinar de Química e Bioloxía (CICA), Rúa as Carballeiras, A Coruña 15071, Spain
[b] Instituto de Investigación Biomédica de A Coruña (INIBIC), Complexo Hospitalario Universitario de A Coruña (CHUAC), Sergas. As Xubias, A Coruña 15006, Spain
[c] Universidade da Coruña, NEUROcom, Facultade de Ciencias da Saúde, Campus de Oza, A Coruña, Spain
[d] Universidade da Coruña, NEUROcom, Facultade de Enfermería e Podoloxía, Campus de Esteiro, Ferrol, Spain
[e] Laboratorio de Neurofisiología Experimental, y Circuitos Neuronales Hospital Nacional de Parapléjicos, Servicio de Salud de Castilla-La Mancha, Toledo, Spain
[f] School of Industrial Engineering, University of Vigo, Campus Universitario Lagoas-Marcosende, Vigo 36310, Spain
[g] Laboratorio de Terapia Celular en Neuropatologías, Centro Andaluz de Biología Molecular y Medicina Regenerativa (CABIMER), Spain
[h] Centro de Estimulación Cerebral de Galicia, Enique Mariñas 32, 15009, A Coruña, Spain

ARTICLE INFO

Keywords:
Non invasive neuromodulation
Dravet
Epilepsy
Magnetic stimulation

ABSTRACT

Dravet syndrome is a rare form of severe genetic epilepsy characterized by recurrent and long-lasting seizures. It appears around the first year of life, with a quick evolution toward an increase in the frequency of the seizures, accompanied by a delay in motor and cognitive development, and does not respond well to antiepileptic medication. Most patients carry a mutation in the gene *SCN1A* encoding the α subunit of the voltage-gated sodium channel Nav1.1, resulting in hyperexcitability of neural circuits and seizure onset. In this work, we applied transcranial static magnetic stimulation (tSMS), a non-invasive, safe, easy-to-use and affordable neuromodulatory tool that reduces neural excitability in a mouse model of Dravet syndrome. We demonstrate that tSMS dramatically reduced the number of crises. Furthermore, crises recorded in the presence of the tSMS were shorter and less intense than in the sham condition. Since tSMS has demonstrated its efficacy at reducing cortical excitability in humans without showing unwanted side effects, in an attempt to anticipate a possible use of tSMS for Dravet Syndrome patients, we performed a numerical simulation in which the magnetic field generated by the magnet was modeled to estimate the magnetic field intensity reached in the cerebral cortex, which could help to design stimulation strategies in these patients. Our results provide a proof of concept for nonpharmacological treatment of Dravet syndrome, which opens the door to the design of new protocols for treatment.

1. Introduction

Dravet Syndrome (DS), also known as Severe Myoclonic Epilepsy of Infancy, is an epileptic encephalopathy first described in 1978 by Dr. Charlotte Dravet (Dravet, 1978) where seizures are considered to contribute to other central nervous system development disorders (Engel and International League Against Epilepsy (ILAE), 2001). DS evolves with motor and cognitive impairments and an elevated risk for sudden unexpected death (Dravet, 2011; Scheffer, 2012). In 2001, DS was associated with a mutation in the sodium channel gene *SCN1A* (Claes et al., 2001), which causes a loss of function of the voltage-gated sodium channel Nav1.1 in inhibitory interneurons. As a consequence, a decrease in inhibitory interneuron function displaces the excitation-inhibition balance to the excitatory side, setting neuronal circuitry closer to the seizure threshold (Ceulemans et al., 2004; Catterall, 2018; Tai et al., 2014). In this condition, different stimuli, from temperature elevation to sensory stimulation, could trigger seizures.

Despite the dramatic consequences for patients and their families, there is no effective treatment for the disease. Pharmacological approaches include cannabinoid agonists (Oakley et al., 2011; Kaplan et al., 2017; Koo et al., 2020; Anderson et al., 2021) and the recently approved compound fenfluramine, an old molecule used as an anorexigenic drug, recovered after being withdrawn from the market because of side effects on the cardiac system (Schoonjans and Ceulemans, 2019;

* Corresponding author at: Universidade da Coruña, NEUROcom, Centro Interdisciplinar de Química e Bioloxía (CICA), Rúa as Carballeiras, A Coruña 15071, Spain.
E-mail address: casto@udc.es (C. Rivadulla).

https://doi.org/10.1016/j.expneurol.2023.114581
Received 19 May 2023; Received in revised form 3 October 2023; Accepted 21 October 2023
Available online 24 October 2023

Odi et al., 2021). The efficacy of these treatments is limited; hence, the search for new therapeutic alternatives continues, and new genetic therapies are being tested in different models (Higurashi et al., 2021; Isom and Knupp, 2021). In this scenario, and in an effort to expand the therapeutic arsenal to fight the disease and control seizures, non-invasive brain stimulation (NIBS) techniques have emerged as a new set of tools with interesting possibilities. Transcranial magnetic stimulation (TMS) and transcranial direct current stimulation (tDCS) have been used to treat epilepsy with mixed results, probably due to the use of different stimulation protocols and the different etiologies of the patients (Cantello et al., 2007; Gschwind and Seeck, 2016). In contrast, tSMS has demonstrated its capacity to systematically reduce neuronal excitability in different experimental models, including humans (Aguila et al., 2016b; Oliviero et al., 2011b; Gonzalez-Rosa et al., 2015; Lozano-Soto et al., 2017; Arias et al., 2017). Furthermore, and very importantly, tSMS has been shown to reduce epileptic activity in different models, including mice, rats, and monkeys (McLean et al., 2003; McLean et al., 2008; Rivadulla et al., 2018).

The aim of this work was to test the effect of tSMS on a mouse model of DS. tSMS has some advantages when compared to the other NIBS techniques; it is cheaper, portable, and easier to use than TMS or tDCS. tSMS allows a spatial configuration to optimally influence large areas of the brain, which is mandatory for the treatment of nonfocal epilepsy such as DS. The data presented in this manuscript show that tSMS dramatically reduces the number and intensity of the crisis evoked by a thermal increase protocol in a DS model. These novel results demonstrate that the application of static magnetic fields might be a very valuable tool to control seizures in human patients. Remarkably, the fact that this technique has already been used in humans without undesirable side effects could speed up the initial phases of clinical trials.

2. Methods

A total of 23 mice, P45 to P60 at the beginning of the experiments, were used in the study. The research was carried out following the rules of the Physiological Spanish Society, the International Council for Laboratory Animal Science, the European Union guidelines (No. 2010/63/EU), and Spanish regulations (Law 6/2013, RD 53/2013, and its modifications in RD 118/2021) for the protection of laboratory animals used for scientific purposes. The ethics committee for animal research of the University Hospital of A Coruña and CABIMER approved the experimental protocols (references P167 and 116/2018, respectively). All efforts were made to minimize animal suffering and the number of animals used, and the 3R rule was applied. Four animals died after the first experimental session and were not included in the analysis, none of them received tSMS.

2.1. Study design

The goal of the study was to evaluate the possible effect of tSMS on epileptic seizures induced by hyperthermia in a mouse model of Dravet syndrome. Heterozygous mice from the B6(Cg)-Scn1atm1.1Dsf/J line (JAX Ref. 026133)(Ricobaraza et al., 2019), carrying a floxed A1783 V mutation for the *Scn1a* gene that affects the domain IV S6 transmembrane region and causes anomalies in channel activity (Kanai et al., 2009), were bred with mice from line Tg(CMV-cre)1Cgn/J (JAX Ref. 006054), which ubiquitously expresses Cre recombinase(Schwenk et al., 1995). The resulting F1 offspring ($Scn1a^{+/A1783V}$; $Cre^{+/-}$) in the mixed C57-B6xBalbC background expressed the A1783 V mutation in all tissues and exhibited high seizure susceptibility and mortality (50% by 16 weeks of age), showing hallmark behavioral and cognitive phenotypes of Dravet syndrome. Experiments were carried out on conditional $Scn1a^{+/A1783V}$; $Cre^{+/-}$ mice ($n = 19$).

ECOG was recorded continuously from 19 anesthetized mice through two copper wires chronically implanted over the dura, and seizure characteristics (intensity, duration, number) were compared between Sham and Magnet conditions. In the first set of animals ($n = 10$), each animal was tested with the Sham or Magnet in alternating sessions; hence, each animal served as its own control. In the second set of mice ($n = 9$), we made 2 groups, Magnet and Sham, and comparisons were made between the groups. In the second set of experiments, the 9 mice were randomly divided into two groups. One of them was exclusively exposed to the real magnet ($n = 4$) and the other to the sham magnet ($n = 5$). Each group underwent eight experimental sessions. Experiments were always performed during the same time period in order to avoid differences due to circadian rhythms.

2.2. Surgical procedure

On the day of surgery, the animals were anesthetized (sevofluorane 3–4%), and two small craniotomies were made over the somatosensory cortex (active electrode) and over the visual cortex (reference). A small wire with an L shape was introduced through each craniotomy and placed on the dura. A drop of fast drying glue was deposited on the cranial surface to prevent the wires from moving and covered by dental cement, maintaining the end of the wires outside the cement. The procedure lasted approximately 30 min, after which buprenorphine (0.1 mg/kg) was subcutaneously administered, and the animals were sent back to their cage to recover for a minimum of 48 h.

2.3. Recording sessions

Animals were anesthetized (sevofluorane 1.5–2%), and ECoG was recorded using an A-M system differential amplifier (Model 1700 A-M System, LLC, Calsborg, WA, USA), digitized at 10 kHz (1401 CED A/D convertor card; Cambridge Electronic Design, UK) and stored (Spike 2 software; Cambridge Electronic Design, UK) in a PC for online checking and posterior analysis.

Since temperature was the trigger for seizures, animals were positioned on a heating pad, with a rectal probe inserted (Thermostatic blanket low noise, model RTC-1, Cibertec, Madrid, Spain) to have a continuous and accurate record of the temperature. Saline solution (0.5 ml) was administered subcutaneously at the beginning and end of the session to restore liquid lost by high temperatures. We started to record ECoG at 37 degrees rectal temperature, and after a period of 5 min (baseline) we placed the Magnet or Sham over the cranium. The metal was as close as possible to the animal but not touching it in order to avoid the wires. We used a cylindrical nickel-plated (Ni–Cu–Ni) NdFeB magnet with a 45-mm diameter and a 30-mm height that weighed 360 g (NEUREK S.L., Toledo Spain). The maximum amount of magnetic energy stored in this magnet was 45 MGOe, with a nominal strength of 765 N (78 kg). Our own measurements showed a magnetic field of 0.5 T next to the magnet and ~0.3 T at 1 cm (Rivadulla et al., 2014). A nonmagnetic replica of identical appearance and weight (i.e., indistinguishable from the magnet) was used for the sham stimulation (NEUREK S.L., Toledo Spain). We used a mechanical arm to place the Magnet or Sham and two small polystyrene pieces on both sides of the animal for support. Thirty minutes after placing the Magnet or the Sham, we started the protocol for triggering crisis by increasing the temperature by means of an infrared lamp that slowly and progressively approached the mouse. Body temperature was continuously increased (0.3 °C/min) from 37 to 42.5 °C, where it was maintained for 5 min. After that, the lamp was withdrawn, and the mouse was cooled until the core temperature returned to 37 °C. In the event that we detected paroxysmal activity in the ECoG during the process of progressively increasing the temperature, we stopped the process, and the animal was maintained at that level for 5 min. The data presented in the paper always refer to the period of 5 min in which the highest temperature that triggered the epileptic seizures was reached. Number of seizures and duration were quantified and compared using a paired *t*-test. Once the animal returned to its normal temperature, it was maintained in a recovery cage alone until behavior returned to normal. Then, the mice were moved to the

cage with other mice. This was considered a "recording session" or "experimental session"; it lasted for approximately 1 h (the recovery time was quite variable, mainly depending on the number and intensity of the crisis), and it was repeated every day.

2.4. Numerical modeling

In this research, the geometric model corresponds with a real mouse brain. It was selected from an open-source online database (Hsu et al., 2021), where an STL model was created from DICOM 3D images. The preparation of the model was carried out using ANSYS SpaceClAim 2020 R1 © software, a computer-aided design tool specially oriented to the repair, simplification and treatment of geometries imported in STL format. In this study, a cell size ranging between 0.2 and 1 mm was created using the ANSYS® meshing preprocessing module. The mouse brain geometry used is shown in Fig. 1-a, the mesh of the simplified brain model is shown in Fig. 1-b, and the full simulated domain, with the main elements identified is shown in Fig. 1-c.

The average skewness was 0.17, and 0.78 was the maximum skewness value. These values guarantee the quality of the mesh. The total number of computational cells was approximately 3 million. The software package ANSYS® v20.2 was used for the simulation. All the walls were set as stationary walls under the no-slip boundary condition. For the resolution of this case, a least squares cell based on the gradient, a first-order spatial discretization setting for magnetic flux density (B) in the X, Y and Z directions, and a least squares cell based on the gradient were used. The simulations were performed under steady conditions, and the magnetization direction was imposed in the normal direction of the flat magnet surface without considering any external magnetic fields. The magnet properties used in the simulation are shown in Table 1.

The simulation was run until the scaled residual of all the variables was below 10^{-4}, according to the ANSYS® convergence criterion recommendation. The simulations were performed on an Intel® Xeon® Processor E5–2697 2.6 GHz cluster with 1280 GB of RAM. The contours of the magnetic field were obtained and analyzed in the brain surface and in the sagittal plane that cuts through the center of the magnet.

2.5. Statistical analysis

To identify ripples, we used a method based on the one described by Simeone et al. (2021)(Simeone et al., 2021). First, the ECoG signal was filtered with an 80–200 Hz zero phase bandpass filter with a stopband attenuation of 60 dB. Then, the root mean square (RMS) of the filtered signal was calculated using a 3 ms sliding window. Relevant peaks (local maxima) in the RMS were detected by comparing them against a threshold (mean RMS + 4 standard deviations). Ripples were defined as oscillations containing at least three consecutive peaks (peaks were considered consecutive if the interval between them was not >30 ms). With this method, for each recording, we calculated the ripple frequency as the total number of ripples divided by the duration of the recording and the ripple duration as the median of the duration of all ripples detected.

Table 1
Neodymium properties.

Property	Value
Density	7600 kg·m^{-3}
Isotropic relative permeability μ_r	1.0997
Magnetic coercivity	900,000 A·m^{-1}
Isotropic electrical conductivity, σ	1555.2 S·m^{-1}

To automatically detect and quantify seizures, spikes and other abnormal signal events in the ECoG, we used a method based on using the line length (LL), or total variation, and wavelet decomposition (Bergstrom et al., 2013). For each of the 63 recording sessions, we first decomposed the ECoG using the Daubechies db4 wavelet. Then, we used the A4 approximation to calculate the LL, defined as the sum of the absolute values of the differences between neighboring data points, over a sliding window (5 s duration) moving in 0.1 s steps. We then calculated the median (LLmed) and standard deviation (LLstdev) of the LL across the 1800 s baseline period. A thresholding factor was derived iteratively by analyzing the baseline ECoG for each recording. It was initially set to 1, and the number of windows in which the LL of the individual baseline recording varied from the LLmed was calculated (see Bergstrom et al., 2013 for details of this procedure). If the number of abnormal events detected along the baseline period was ≥1, the thresholding factor was increased by 0.5, and the process was repeated until the number of abnormal events during the baseline was equal. Finally, we compared the LLs obtained along each recording against each individual thresholding factor to identify abnormal events. The percentage of windows with abnormal events after the baseline period was obtained for all 63 sessions. Magnet and sham recordings were compared using an unpaired *t*-test with Welch's correction.

3. Results

3.1. tSMS reaches the cerebral cortex with an intensity of 0.2–0.3 Tesla

To estimate the intensity and extension of the magnetic field that the brains of the mice received during the experiments, a numerical simulation was carried out. In this simulation, the magnetic field generated by the magnet was modeled, reproducing the same boundary conditions that were used in the experiments (see Methods).

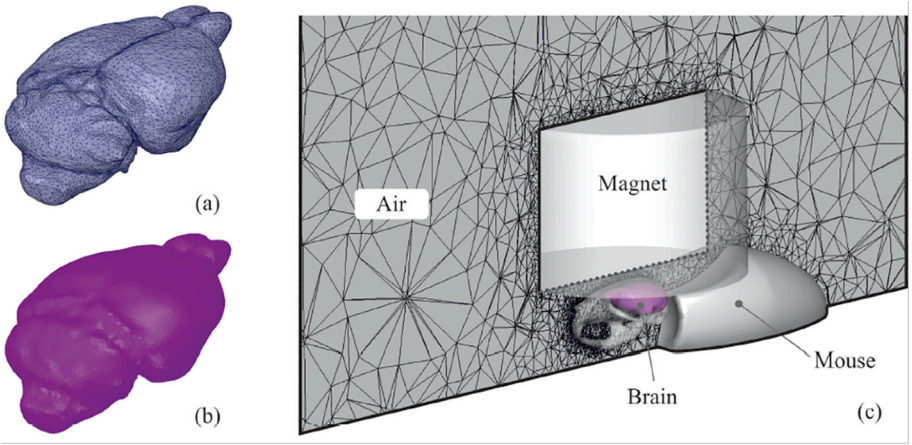

Fig. 1. Modeling domain of the mouse brain. Mesh details: (a) STL geometry of the mouse's brain. (b) Mesh of the simplified geometry. (c) Modeling domain.

Fig. 2 shows the contours of the magnetic flux. The intensity of the magnetic field decreases in the radial direction, when moving away from the axis of the magnet, but decreases much faster when moving away from its surface, in the magnet axis direction, as shown in Fig. 2a. This rapid decrease in the magnetic field intensity results in a range of values inside the brain between 0.2 and 0.4 Tesla, seen in Fig. 2b. The use of this modeling tool could be valuable in estimating, prior to clinical trials, the penetration of the magnetic field and the distribution on different depths of the brain.

3.2. tSMS reduced the number, intensity, and duration of seizures

In an initial set of animals, $n = 10$, tSMS or sham was applied on alternating days (in a randomized order), which allowed us to compare the effect of tSMS on each individual. During the protocol (see Methods), body temperature was increased up to 42.5 degrees or to the level where the first seizure was detected in the online electrocorticogram (ECoG) and then maintained for 300 s before being decreased.

Fig. 3 shows the raw EcoG signal recorded from the same mouse (identified as number 32) on two consecutive days, corresponding to sham (A) or tSMS (B) sessions, and the corresponding spectrograms for the same period, showing instant frequencies. Four hundred seconds of recordings are shown in each case, including those 5 min where the temperature was above 42 °C degrees. During the sham condition, the recorded EcoG shows clear paroxysmal activity, indicated by blue arrows in the figure, during which several epileptic morphologies could be detected, including sharp waves, spike waves or polyspikes, visible on the expanded trace below the spectrogram (*). During these seizures, instant frequencies up to 500 Hz were usually recorded, and by the end of the sessions, a late component (marked by a black arrow in the recording and expanded below **) characterized by slow waves with a frequency of approximately 0,5 Hz was observed. During the tSMS (B), no seizure activity was detected in this session; however, the EcoG was not normal, and some epileptic-like activity (*) was detected corresponding to a 0.2 Hz oscillation that could indicate some kind of preictal activity that was not able to trigger the seizure.

There was some variability in the behavior of each individual during sham sessions, with some having one or two long duration paroxysmal episodes per session and others having up to 10 short episodes. We observe a tendency to evolve toward a daily increase in the number and intensity of crises, as if the induction of crisis somehow made the brain more suitable to trigger seizures, but in any case, the magnet was able to reduce those numbers. Fig. 4A represents the number of seizures for each animal in both conditions. All mice but one (which did not change) showed a reduction in the number of seizures. The case of three animals whose seizures disappeared completely in the presence of the magnet is noticeable. On average, the number of seizures fell by 60% in the presence of the magnet, from 9.82 ± 5.1 (mean ± SD) to 3.9 ± 2.6. $P <$ 0.01 *t*-test for paired samples. The reduction in the number of seizures was accompanied by a reduction in the duration of the seizures from 28.1 ± 16 s in Sham to 19.66 ± 8 s in the magnet condition, Fig. 4B (31% reduction, $P < 0.05$ t-test). Taken together, the reduction in the number of seizures and the decrease in the duration resulted in a decrease by 72.2% of the time that the animals spent in seizures (4C).

3.3. Repeated application of tSMS improved the results

In a second set of *Scn1a*$^{+/A1783V}$ mice ($n = 9$), we divided them into two experimental groups: Magnet ($n = 4$), in which the thermal protocol was always applied in the presence of tSMS, and Sham ($n = 5$), in which the same thermal protocol was always applied with the Sham, so the animals in the Sham group never received tSMS. Up to 8 recording sessions were made for each animal (see methods). All the parameters evaluated were clearly better in the Magnet group. The probability of having at least one seizure in a given session was 92% in the Sham animals versus 48% in the Magnet group, and the average duration of the seizures was shorter in the Magnet animals (12.69 ± 4.5 s) (Fig. 5A) versus the sham (25.7 ± 7 s) group. This, together with the decrease in the number of seizures, resulted in a reduction of 86% of the total time that the animal spent in seizures (Fig. 5B). We analyzed the temperature at which the first seizure was detected, but the differences were not significant for this parameter: 42.22 ± 0.65 °C for the sham versus 42.12 ± 0.42 for the magnet.

In this set of animals, we ran an automated analysis based on Bergstrom et al., 2013 (Bergstrom et al., 2013) (see methods for details) that was able to detect abnormal events during the recording sessions following an individual baseline calibration for each session. On average, during the recording sessions in which the tSMS was applied ($n = 29$), the proportion of abnormal events was 0.008 ($SD = 0.014$), while during the sham sessions ($n = 34$), the average proportion was 0.078 ($SD = 0.072$). The probability for abnormal events in the ECoG increased by 12.3 times in animals exposed to the sham compared with the magnet group. These values are represented in Fig. 5C.

Mice exposed to real tSMS suffered milder paroxysmal episodes than sham mice, which can be observed from the seizures recorded in the sham group, as shown in Fig. 6A. High frequencies easily extended up to 500 Hz on the spectrogram analysis of instantaneous frequencies; these values were not reached in the magnet condition (Fig. 6B). Considering that the appearance of high frequencies in the ECoG, in the range of ripples, are indicators of seizure severity (Schönberger et al., 2019), we analyzed the presence of ripples (80 to 200 Hz) in both conditions (see methods). Fig. 6C graphically represents those results. The left panel shows a segment of the raw ECoG (top) and after the 80–200 filtering (bottom) where a ripple can be seen. On average, during the recording sessions in which the magnet was applied (n = 29), the ripple frequency was 0.25 ripples/s (SD = 0.08), and the ripple duration was 0.025 s (SD

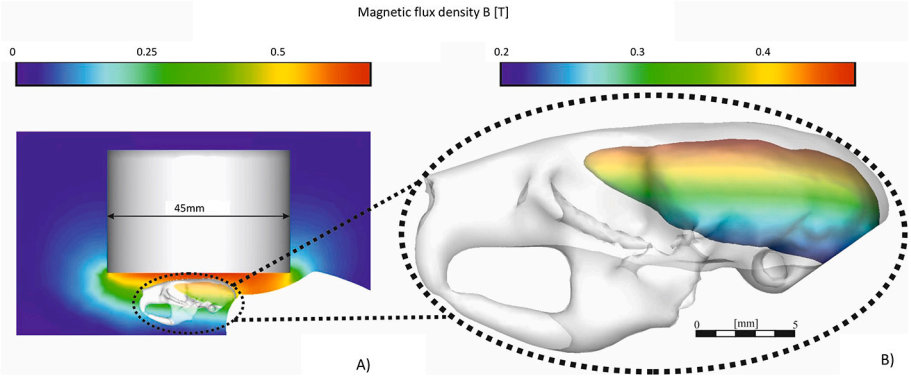

Fig. 2. Contours of the magnetic field in the mouse brain. (a) General view of the simulated domain. (b) Brain zone detailed view. The distance from the magnet to the skin of the animal was approximately 2 mm to avoid contact with the recording wires, which is not represented in the figure.

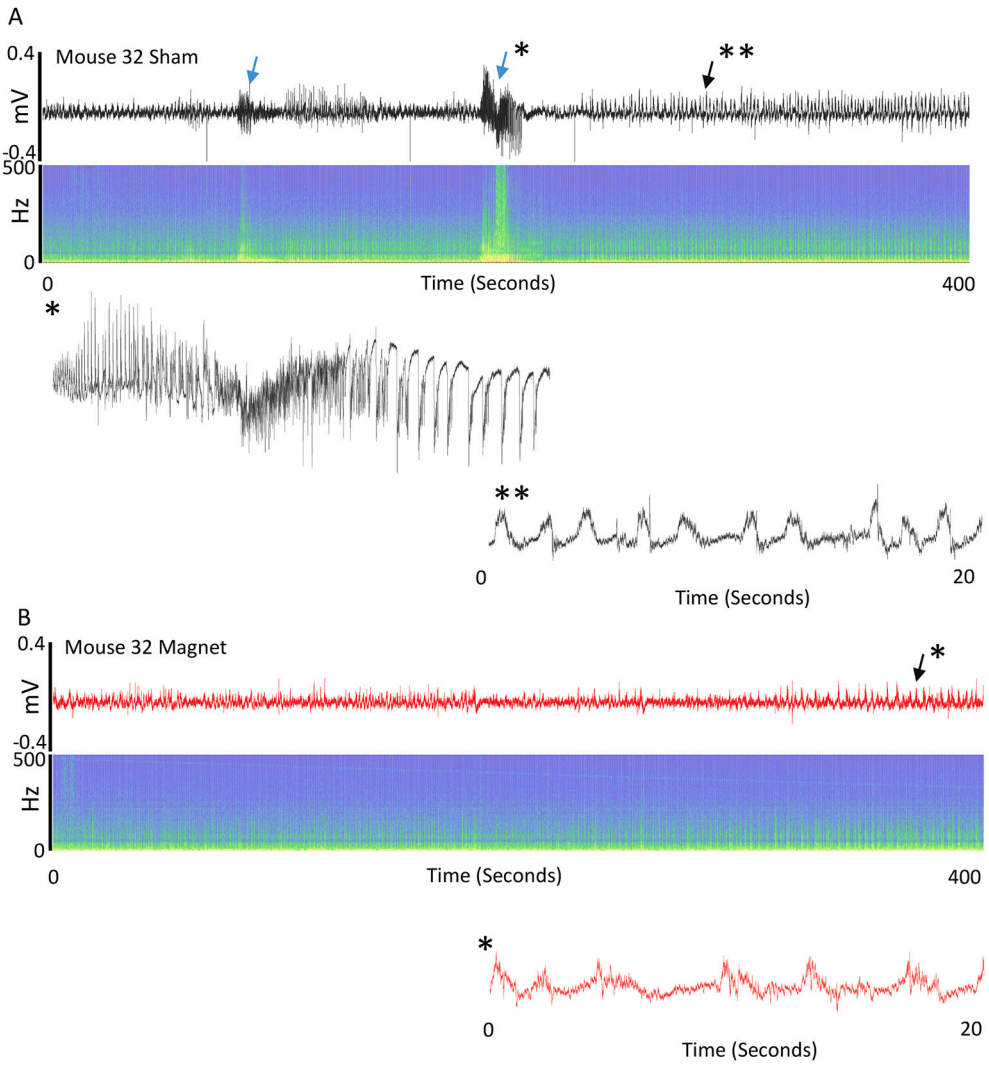

Fig. 3. Acute application of tSMS during the thermal increase protocol significantly decreased the number of recorded seizures. EcoG records obtained from the same mouse (#32) on two consecutive days, reaching exactly the same temperature, 42,3 °C. A Sham, B Real magnet. Blue arrows mark paroxysmal activity, only present in the sham condition, black arrows indicate periods characterized by slow waves. Sections marked with * or ** in the recordings are expanded. See the text for further details. (For interpretation of the references to colour in this figure legend, the reader is referred to the web version of this article.)

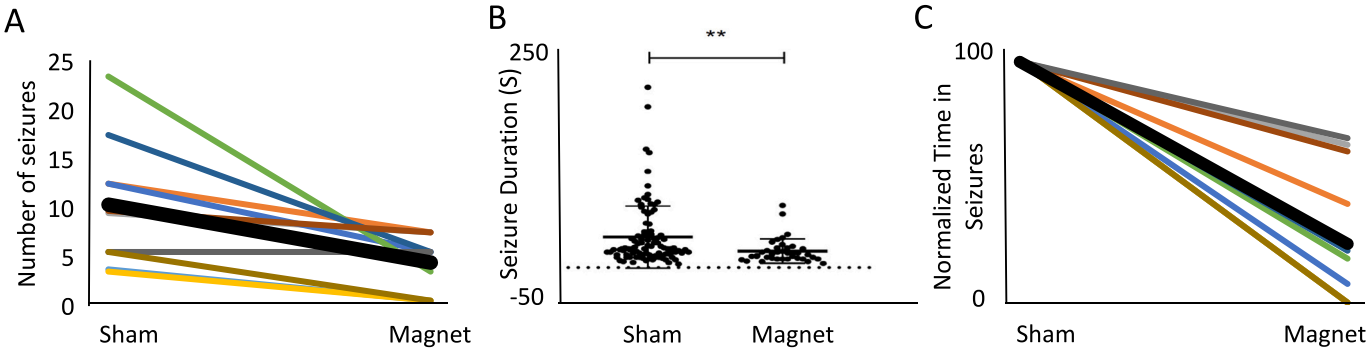

Fig. 4. The number and duration of seizures were reduced in the presence of the magnet. A) Diagram comparing the number of seizures developed for each animal in both experimental conditions: Sham and Magnet. The black thick line represents the averaged values, $p < 0.01$, *t*-test. B) Duration of seizures in both conditions, each dot represents an individual seizure, the horizontal lines indicate the mean, and the error bars indicate the SD, $p < 0.01$, t-test. C) Diagram comparing the time that each animal spent "in seizures" during the Sham and the Magnet sessions, $p < 0.01$, t-test.

= 0.004). During the sham sessions the average frequency was 0.33 ripples/s (SD = 0.09), and the average duration was 0.026 s (SD = 0.004) (n = 34). The difference in frequency, represented in Fig. 6C center, was statistically significant (t(61) = 3.945, $p < 0.0005$), while the difference in duration, represented in Fig. 6C right, was not significant (t(59) = 1.12, $p = 0.227$).

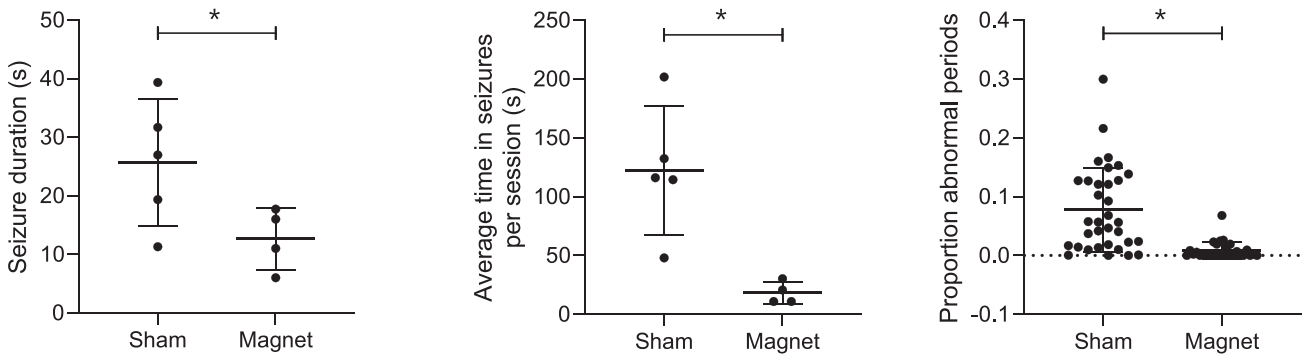

Fig. 5. tSMS reduces seizure duration. A) Average duration of seizures in the sham group and the magnet group, each dot represents the average value for individual mouse, $p < 0.01$, t-test. B) Average time that the animals spent in seizure per session in both experimental conditions, again each dot represents the values for each animal, $p < 0.01$, t-test. C) Proportion of windows with abnormal events detected in the sham and magnet sessions. Each dot represents an individual recording session, the horizontal lines indicate the mean, and the error bars indicate the SD, $t(36) = 5.505$; $p < 0.0001$.

4. Discussion

Our results show that tSMS, a non-invasive neuromodulatory technique, can reduce the number, duration, and severity of crises in a mouse model of DS. We tested the effect of tSMS in 2 groups of animals. In the first group, the crisis was induced in the same animals alternatively in the presence of the magnet or the sham, while the second set of animals was separated: 5 were always under the sham condition, and 4 were always under the magnet. In both groups, the results were similar, with a dramatic reduction of 72% and 86% of the time than the animals were in seizures for the magnet condition compared to the sham. Automatic analysis of the ECOG signal reported a 12.3 times higher probability of detecting abnormal events in the sham group than in the magnet group.

DS begins with seizures that tend to evolve with age and is associated with a myriad of symptoms, including motor and cognitive deficits, sleep disturbances, and an increased risk of death in early childhood (Cooper et al., 2016; Brunklaus et al., 2012). There is no pharmacological treatment capable of controlling crises in DS, even though the results of new drugs (cannabidiol, fenfluramine or stiripentol) are promising, and reductions in the number of crises up to 50% have been achieved in a significant number of patients (Wirrell and Nabbout, 2019). It is important to note that in our experiments, in a murine model, the seizure reduction figures were much higher, approximately 86%, which makes tSMS a solid alternative for clinical trials. In particular, it has been shown that the use of tSMS in healthy humans is free of undesirable effects. In the vast majority of DS cases (~80%), the preponderant alteration is a loss of function of the voltage-gated sodium channels (Nav1.1). This functional deficit critically affects cortical GABAergic interneurons, altering inhibitory control and producing an abnormal increase in excitation. It is precisely here that tSMS can play a decisive role. We do not know the exact mechanism of tSMS (see below), but we have consistent evidence that it reduces cortical excitability: tSMS reduces the motor evoked potential in humans(Oliviero et al., 2011b), reduces performance in a visual detection task in primates and humans (Gonzalez-Rosa et al., 2015; Aguila et al., 2016b), and reduces photophobia symptoms (Lozano-Soto et al., 2017). Furthermore, in a previous study, we demonstrated that tSMS can reduce epileptic activity in two different experimental models; a pharmacological model in rats and a traumatic model in primates (Rivadulla et al., 2018). The results discussed here are compatible with this idea and strongly suggest that tSMS would reduce cortical excitability, maintaining cortical circuits far away from the threshold level for seizures. Even when the system reaches this threshold, the intensity of the seizures is lower in the presence of the magnet, perhaps because the number of neurons involved is lower. Experiments were performed in anesthetized animals which allow us to have a better control on the temperature, and characterize crisis, however it implies a clear limitation of the study since we do not observe the effect on spontaneous seizures and we did not observe behavioral changes. Experiments addressing those issues are being planned. Regarding the use of sevofluorane as anesthetic, it has been shown to increase epileptiform activity (Gibert et al., 2012; Iijima et al., 2000), this would play against our interest since it could be reducing the effectiveness of the tSMS, that could be even higher with other anesthetics or in awake conditions.

As we pointed out above, the mechanism through which tSMS produces its effects has not yet been fully explained. It has been shown that magnetic fields in the range we used are able to produce physical changes at the cell membrane that can distort imbedded ion channels sufficiently to alter their function (Rosen, 2003a). This mechanism would be supported by studies demonstrating abnormal functioning of voltage-gated ion channels under a static magnetic field (Rosen, 1993, 2003b). Mechanical stretching of the membrane has also been theoretically proposed (Hernando et al., 2020) as a possible mechanism that explains the observed effects. Finally, it has been recently proposed that the magnet could act on the Lorentz force of the ions flowing through the ion channels; small increases could introduce an additional friction between ions and channel walls, reducing the conductance (Freire et al., 2020).

We used neodymium magnets (45 mm diameter) with a magnetic field strength of 0.5 T and a continuous exposure time of approximately 45 min. This kind of magnet has been previously used for humans, and it could be considered too large for mice. However, in the mouse model we are trying to modulate activity in the whole cortex, while in previous studies in humans, the goal was to modulate a specific area. The numerical model calculates a magnetic field intensity between 0,2 and 0,4 T at different cortical areas in our experiments in mice. We are using just 1 magnetic source and the intensity decays with distance being clearly higher in the dorsal cortex (next to the magnet) than in the inferior temporal lobe for instance. Thinking about a possible translation of the therapy to children with DS, it would be necessary to work on the design of helmets capable of accommodating several magnets to create homogeneous magnetic fields over large cortical areas. For this purpose, numerical models can be a very valuable tool in the configuration of magnetic positions. The desired intensity at the cerebral cortex is between 120 and 200 mT. This has been calculated as the approximate intensity that is achieved when this magnet was applied at the human scalp, which has previously been demonstrated to be effective and safe (Oliviero et al., 2011a; Gonzalez-Rosa et al., 2015; Lozano-Soto et al., 2017; Oliviero et al., 2015; Aguila et al., 2016a; Rivadulla et al., 2018). Regarding safety, the conditions used in this experiment would be far from the limits recommended by the World Health Organization (WHO); that is, the "time-weighted average of 200 mT during the working day for occupational exposure". Nevertheless, safety is a main issue for a new

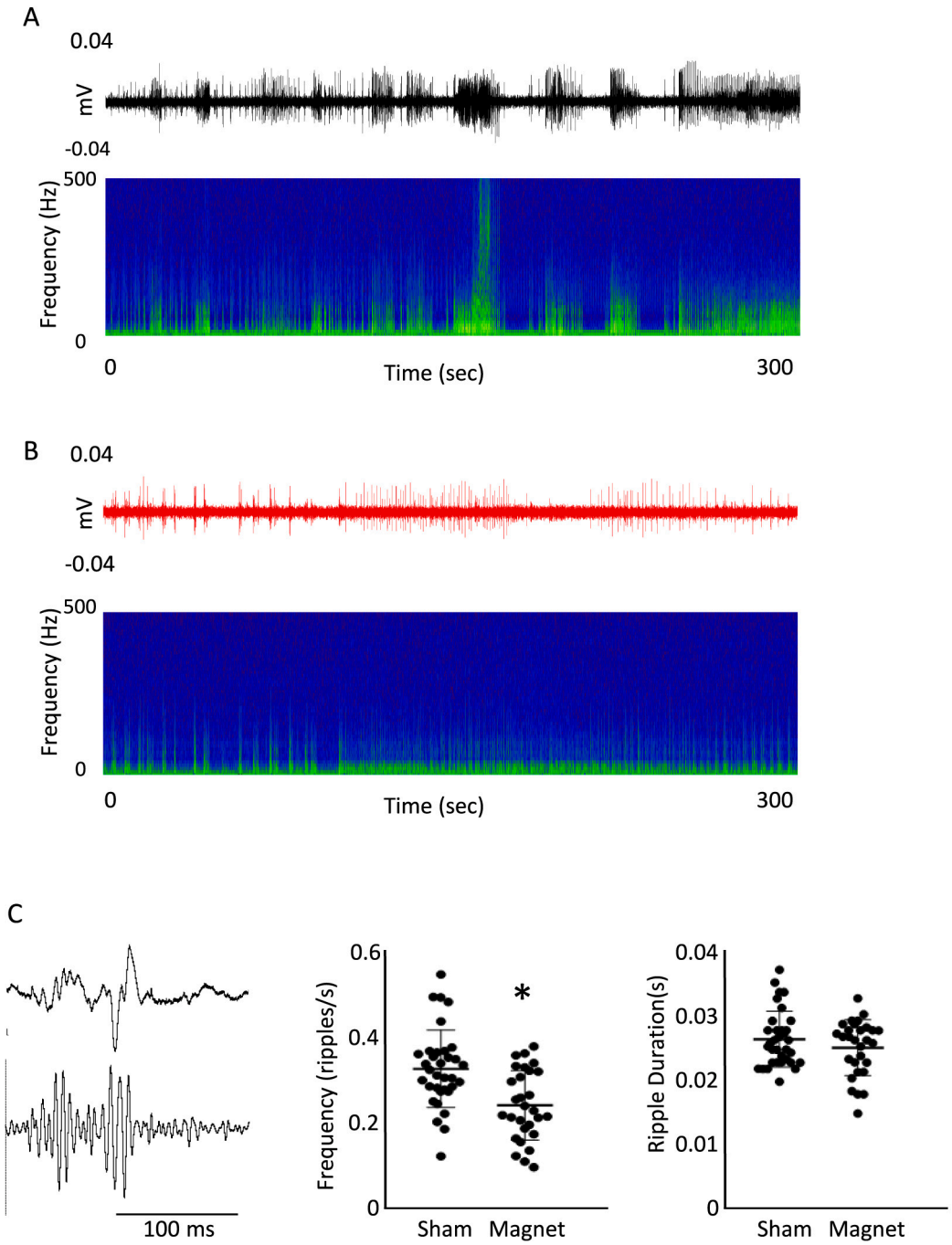

Fig. 6. Acute application of tSMS reduces high-frequency signals in the ECoG. ECoG recordings and spectrograms obtained from two experimental animals from the Sham (A) and Magnet (B) groups at similar stages of treatment. C) Ripple analysis, left: ECoG trace before (top) and after bandpass (80–200 Hz) filtering (bottom), center: averaged ripple frequency in the different experimental conditions ($p < 0.01$), right: averaged ripple duration ($p > 0.01$).

neuromodulatory tool before it is used as a clinical tool; hence, future studies are needed to assess the incidence of possible adverse effects among a large cohort of subjects who receive specific tSMS protocols.

Another important issue when planning a translation to humans is to find specific guidelines for magnet exposure. We demonstrate here that the magnet can reduce crisis intensity in the worst possible scenario since we push seizures to appear by increasing the temperature. This could be a treatment for children who are going to experience a well-known stressful situation with the ability to trigger a crisis, but ideally, the magnet should be a chronic treatment used to reduce cortical excitability and keep it low, decreasing the probability of reaching the threshold for seizures; hence, we consider that reaching intensities up to 0,4 T as obtained in mice would not be needed, or could be compensated with larger exposition times. This is theoretical, hence the difficulty in reaching those intensities in the human brain is a potential limitation for translating the results to patients.

5. Conclusions

Considering the results that we have presented and those obtained by other authors, we believe that tSMS is emerging as an affordable, simple, safe and promising therapy for Dravet patients, alone or complementing the partial effectiveness that has been obtained with other treatments.

Author contributions

Conceptualization: CR, JA, JC.
Methodology MAD.
Investigation: CdL and CR.
Software: ES and CP.
Formal Analysis: CR, JPV, CdL, JC.
Writing – original draft: CR.
All authors revised the manuscript for important intellectual content and read and approved the final manuscript.

Declaration of Competing Interest

The authors declare that they have no competing financial interests.

Data availability

All data and materials used in the analysis will be made available on request for proposals that set out to achieve aims specified in a methodologically and scientifically sound protocol. Applications to access data can be sent to casto@udc.es. Data access will be used for noncommercial, academic, and research use only.

Acknowledgments

Funding
Instituto de salud Carlos III (ISCIII) PI21/00151, co-funded by the European Union
Xunta de Galicia, Grupos de referencia competitiva 2021 ED431C 2022/05 (CR)
Ministerio de Ciencia e Innovacion PID2019-108250RJ-100
Xunta de Galicia, Grupos con Pontencial Crecimiento 2021 (JPV).
Apoyo Dravet (MAD).
JPV has a contract under the Ramon y Cajal program (RYC2019–026380-I).

References

Aguila, J., Cudeiro, J., Rivadulla, C., 2016a. Effects of static magnetic fields on the visual cortex: reversible visual deficits and reduction of neuronal activity. Cereb. Cortex 26 (2), 628–638. https://doi.org/10.1093/cercor/bhu228.

Aguila, Jordi, Cudeiro, Javier, Rivadulla, Casto, 2016b. Effects of static magnetic fields on the visual cortex: reversible visual deficits and reduction of neuronal activity. Cereb. Cortex 26 (2), 628–638. https://doi.org/10.1093/cercor/bhu228.

Anderson, L.L., Doohan, P.T., Hawkins, N.A., Bahceci, D., Thakur, G.A., Kearney, J.A., Arnold, J.C., 2021. The endocannabinoid system impacts seizures in a mouse model of Dravet syndrome. Neuropharmacology 108897. https://doi.org/10.1016/j.neuropharm.2021.108897.

Arias, P., Adán-Arcay, L., Puerta-Catoira, B., Madrid, A., Cudeiro, J., 2017. Transcranial static magnetic field stimulation of M1 reduces corticospinal excitability without distorting sensorimotor integration in humans. Brain Stimul. 10 (2), 340–342. https://doi.org/10.1016/j.brs.2017.01.002.

Bergstrom, R.A., Choi, J.H., Manduca, A., Shin, H.S., Worrell, G.A., Howe, C.L., 2013. Automated identification of multiple seizure-related and interictal epileptiform event types in the EEG of mice. Sci. Rep. 3, 1483. https://doi.org/10.1038/srep01483.

Brunklaus, A., Ellis, R., Reavey, E., Forbes, G.H., Zuberi, S.M., 2012. Prognostic, clinical and demographic features in SCN1A mutation-positive Dravet syndrome. Brain 135 (Pt 8), 2329–2336. https://doi.org/10.1093/brain/aws151.

Cantello, R., Rossi, S., Varrasi, C., Ulivelli, M., Civardi, C., Bartalini, S., Vatti, G., Cincotta, M., Borgheresi, A., Zaccara, G., Quartarone, A., Crupi, D., Laganà, A., Inghilleri, M., Giallonardo, A.T., Berardelli, A., Pacifici, L., Ferreri, F., Tombini, M., Gilio, F., Quarato, P., Conte, A., Manganotti, P., Bongiovanni, L.G., Monaco, F., Ferrante, D., Rossini, P.M., 2007. Slow repetitive TMS for drug-resistant epilepsy: clinical and EEG findings of a placebo-controlled trial. Epilepsia 48 (2), 366–374. https://doi.org/10.1111/j.1528-1167.2006.00938.x.

Catterall, W.A., 2018. Dravet syndrome: a Sodium Channel Interneuronopathy. Curr. Opin. Physiol. 2, 42–50. https://doi.org/10.1016/j.cophys.2017.12.007.

Ceulemans, B.P., Claes, L.R., Lagae, L.G., 2004. Clinical correlations of mutations in the SCN1A gene: from febrile seizures to severe myoclonic epilepsy in infancy. Pediatr. Neurol. 30 (4), 236–243. https://doi.org/10.1016/j.pediatrneurol.2003.10.012.

Claes, L., Del-Favero, J., Ceulemans, B., Lagae, L., Van Broeckhoven, C., De Jonghe, P., 2001. De novo mutations in the sodium-channel gene SCN1A cause severe myoclonic epilepsy of infancy. Am. J. Hum. Genet. 68 (6), 1327–1332. https://doi.org/10.1086/320609.

Cooper, M.S., Mcintosh, A., Crompton, D.E., McMahon, J.M., Schneider, A., Farrell, K., Ganesan, V., Gill, D., Kivity, S., Lerman-Sagie, T., McLellan, A., Pelekanos, J., Ramesh, V., Sadleir, L., Wirrell, E., Scheffer, I.E., 2016. Mortality in Dravet syndrome. Epilepsy Res. 128, 43–47. https://doi.org/10.1016/j.eplepsyres.2016.10.006.

Dravet, C., 1978. Les Epilepsies graves de l'enfant. Vie Medic. 8, 6.

Dravet, C., 2011. The core Dravet syndrome phenotype. Epilepsia 52 (Suppl. 2), 3–9. https://doi.org/10.1111/j.1528-1167.2011.02994.x.

Engel, J., International League Against Epilepsy (ILAE), 2001. A proposed diagnostic scheme for people with epileptic seizures and with epilepsy: report of the ILAE task force on classification and terminology. Epilepsia 42 (6), 796–803. https://doi.org/10.1046/j.1528-1157.2001.10401.x.

Freire, M.J., Bernal-Méndez, J., Pérez, A.T., 2020. The Lorentz force on ions in membrane channels of neurons as a mechanism for transcranial static magnetic stimulation. Electromagn. Biol. Med. 39 (4), 310–315. https://doi.org/10.1080/15368378.2020.1793172.

Gibert, S., Sabourdin, N., Louvet, N., Moutard, M.L., Piat, V., Guye, M.L., Rigouzzo, A., Constant, I., 2012. Epileptogenic effect of sevoflurane: determination of the minimal alveolar concentration of sevoflurane associated with major epileptoid signs in children. Anesthesiology 117 (6), 1253–1261. https://doi.org/10.1097/ALN.0b013e318273e272.

Gonzalez-Rosa, J.J., Soto-Leon, V., Real, P., Carrasco-Lopez, C., Foffani, G., Strange, B.A., Oliviero, A., 2015. Static magnetic field stimulation over the visual cortex increases alpha oscillations and slows visual search in humans. J. Neurosci. 35 (24), 9182–9193. https://doi.org/10.1523/JNEUROSCI.4232-14.2015.

Gschwind, M., Seeck, M., 2016. Transcranial direct-current stimulation as treatment in epilepsy. Expert. Rev. Neurother. 16 (12), 1427–1441. https://doi.org/10.1080/14737175.2016.1209410.

Hernando, A., Galvez, F., García, M.A., Soto-León, V., Alonso-Bonilla, C., Aguilar, J., Oliviero, A., 2020. Effects of moderate static magnetic field on neural systems is a non-invasive mechanical stimulation of the brain possible theoretically? Front. Neurosci. 14, 419. https://doi.org/10.3389/fnins.2020.00419.

Higurashi, N., Broccoli, V., Hirose, S., 2021. Genetics and gene therapy in Dravet syndrome. Epilepsy Behav. 108043. https://doi.org/10.1016/j.yebeh.2021.108043.

Hsu, Li-Ming, Ban, Woomi, Chao, Tzu-Hao, Song, Sheng, Hayden, Domenic, Lindsay, Cerri, Margaret, Walton, Sung-Ho, Broadwater, Ian, Lee Yenyu, 2021. CAMRI Mouse Brain MRI Data (OpenNeuro).

Iijima, T., Nakamura, Z., Iwao, Y., Sankawa, H., 2000. The epileptogenic properties of the volatile anesthetics sevoflurane and isoflurane in patients with epilepsy. Anesth. Analg. 91 (4), 989–995. https://doi.org/10.1097/00000539-200010000-00041.

Isom, L.L., Knupp, K.G., 2021. Dravet syndrome: novel approaches for the Most common genetic epilepsy. Neurotherapeutics 18 (3), 1524–1534. https://doi.org/10.1007/s13311-021-01095-6.

Kanai, K., Yoshida, S., Hirose, S., Oguni, H., Kuwabara, S., Sawai, S., Hiraga, A., Fukuma, G., Iwasa, H., Kojima, T., Kaneko, S., 2009. Physicochemical property changes of amino acid residues that accompany missense mutations in SCN1A affect epilepsy phenotype severity. J. Med. Genet. 46 (10), 671–679. https://doi.org/10.1136/jmg.2008.060897.

Kaplan, J.S., Stella, N., Catterall, W.A., Westenbroek, R.E., 2017. Cannabidiol attenuates seizures and social deficits in a mouse model of Dravet syndrome. Proc. Natl. Acad. Sci. U. S. A. 114 (42), 11229–11234. https://doi.org/10.1073/pnas.1711351114.

Koo, C.M., Kim, S.H., Lee, J.S., Park, B.J., Lee, H.K., Kim, H.D., Kang, H.C., 2020. Cannabidiol for treating Lennox-Gastaut syndrome and Dravet syndrome in Korea. J. Korean Med. Sci. 35 (50), e427 https://doi.org/10.3346/jkms.2020.35.e427.

Lozano-Soto, E., Soto-León, V., Sabbarese, S., Ruiz-Alvarez, L., Sanchez-Del-Rio, M., Aguilar, J., Strange, B.A., Foffani, G., Oliviero, A., 2017. Transcranial static magnetic field stimulation (tSMS) of the visual cortex decreases experimental photophobia. Cephalalgia. https://doi.org/10.1177/0333102417736899, 333102417736899.

McLean, M.J., Engström, S., Holcomb, R.R., Sanchez, D., 2003. A static magnetic field modulates severity of audiogenic seizures and anticonvulsant effects of phenytoin in DBA/2 mice. Epilepsy Res. 55 (1–2), 105–116. https://doi.org/10.1016/s0920-1211(03)00109-8.

McLean, M.J., Engström, S., Qinkun, Z., Spankovich, C., Polley, D.B., Polley, D., 2008. Effects of a static magnetic field on audiogenic seizures in black Swiss mice. Epilepsy Res. 80 (2–3), 119–131. https://doi.org/10.1016/j.eplepsyres.2008.03.022.

Oakley, J.C., Kalume, F., Catterall, W.A., 2011. Insights into pathophysiology and therapy from a mouse model of Dravet syndrome. Epilepsia 52 (Suppl. 2), 59–61. https://doi.org/10.1111/j.1528-1167.2011.03004.x.

Odi, R., Invernizzi, R.W., Gallily, T., Bialer, M., Perucca, E., 2021. Fenfluramine repurposing from weight loss to epilepsy: what we do and do not know. Pharmacol. Ther. 226, 107866 https://doi.org/10.1016/j.pharmthera.2021.107866.

Oliviero, A., Mordillo-Mateos, L., Arias, P., Panyavin, I., Foffani, G., Aguilar, J., 2011a. Transcranial static magnetic field stimulation of the human motor cortex. J. Physiol. 589 (Pt 20), 4949–4958. https://doi.org/10.1113/jphysiol.2011.211953.

Oliviero, A., Mordillo-Mateos, L., Arias, P., Panyavin, I., Foffani, G., Aguilar, J., 2011b. Transcranial static magnetic field stimulation of the human motor cortex. J. Physiol.-London 589 (20), 4949–4958. https://doi.org/10.1113/jphysiol.2011.211953.

Oliviero, A., Carrasco-López, M.C., Campolo, M., Perez-Borrego, Y.A., Soto-León, V., Gonzalez-Rosa, J.J., Higuero, A.M., Strange, B.A., Abad-Rodriguez, J., Foffani, G., 2015. Safety study of transcranial static magnetic field stimulation (tSMS) of the human cortex. Brain Stimul. 8 (3), 481–485. https://doi.org/10.1016/j.brs.2014.12.002.

Ricobaraza, A., Mora-Jimenez, L., Puerta, E., Sanchez-Carpintero, R., Mingorance, A., Artieda, J., Nicolas, M.J., Besne, G., Bunuales, M., Gonzalez-Aparicio, M., Sola-

Sevilla, N., Valencia, M., Hernandez-Alcoceba, R., 2019. Epilepsy and neuropsychiatric comorbidities in mice carrying a recurrent Dravet syndrome SCN1A missense mutation. Sci. Rep. 9 (1), 14172. https://doi.org/10.1038/s41598-019-50627-w.

Rivadulla, C., Foffani, G., Oliviero, A., 2014. Magnetic field strength and reproducibility of neodymium magnets useful for transcranial static magnetic field stimulation of the human cortex. Neuromodulation 17 (5), 438–441 discussion 441-2. https://doi.org/10.1111/ner.12125.

Rivadulla, C., Aguilar, J., Coletti, M., Aguila, J., Prieto, S., Cudeiro, J., 2018. Static magnetic fields reduce epileptiform activity in anesthetized rat and monkey. Sci. Rep. 8 (1), 15985. https://doi.org/10.1038/s41598-018-33808-x.

Rosen, A.D., 1993. Membrane response to static magnetic fields: effect of exposure duration. Biochim. Biophys. Acta 1148 (2), 317–320.

Rosen, A.D., 2003a. Effect of a 125 mT static magnetic field on the kinetics of voltage activated Na+ channels in GH3 cells. Bioelectromagnetics 24 (7), 517–523. https://doi.org/10.1002/bem.10124.

Rosen, A.D., 2003b. Mechanism of action of moderate-intensity static magnetic fields on biological systems. Cell Biochem. Biophys. 39 (2), 163–173. https://doi.org/10.1385/CBB:39:2:163.

Scheffer, I.E., 2012. Diagnosis and long-term course of Dravet syndrome. Eur. J. Paediatr. Neurol. 16 (Suppl. 1), S5–S8. https://doi.org/10.1016/j.ejpn.2012.04.007.

Schönberger, J., Birk, N., Lachner-Piza, D., Dümpelmann, M., Schulze-Bonhage, A., Jacobs, J., 2019. High-frequency oscillations mirror severity of human temporal lobe seizures. Ann. Clin. Transl. Neurol. 6 (12), 2479–2488. https://doi.org/10.1002/acn3.50941.

Schoonjans, A.S., Ceulemans, B., 2019. An old drug for a new indication: repurposing Fenfluramine from an Anorexigen to an antiepileptic drug. Clin. Pharmacol. Ther. 106 (5), 929–932. https://doi.org/10.1002/cpt.1469.

Schwenk, F., Baron, U., Rajewsky, K., 1995. A cre-transgenic mouse strain for the ubiquitous deletion of loxP-flanked gene segments including deletion in germ cells. Nucleic Acids Res. 23 (24), 5080–5081. https://doi.org/10.1093/nar/23.24.5080.

Simeone, T.A., Heruye, S.H., Kostansek, J.A., Yeh, M.Y., Matthews, S.A., Samson, K.K., Simeone, K.A., 2021. Carbamazepine reduces sharp wave-ripple complexes and exerts synapse-specific inhibition of neurotransmission in ex vivo hippocampal slices. Brain Sci. 11 (6) https://doi.org/10.3390/brainsci11060787.

Tai, C., Abe, Y., Westenbroek, R.E., Scheuer, T., Catterall, W.A., 2014. Impaired excitability of somatostatin- and parvalbumin-expressing cortical interneurons in a mouse model of Dravet syndrome. Proc. Natl. Acad. Sci. U. S. A. 111 (30), E3139–E3148. https://doi.org/10.1073/pnas.1411131111.

Wirrell, E.C., Nabbout, R., 2019. Recent advances in the drug treatment of Dravet syndrome. CNS Drugs 33 (9), 867–881. https://doi.org/10.1007/s40263-019-00666-8.